Molecular Determinants of the Reversible Membrane Anchorage of the G-Protein Transducin †

ARTICLE *in* BIOCHEMISTRY · JULY 1999

Impact Factor: 3.02 · DOI: 10.1021/bi990298+ · Source: PubMed

6 AUTHORS, INCLUDING:

Klaus Peter Hofmann
Charité Universitätsmedizin Berlin
201 PUBLICATIONS **9,913** CITATIONS
SEE PROFILE

Anna Seelig
University of Basel
79 PUBLICATIONS **5,683** CITATIONS
SEE PROFILE

Molecular Determinants of the Reversible Membrane Anchorage of the G-Protein Transducin†

Harald R. Seitz,‡ Martin Heck,‡ Klaus Peter Hofmann,‡ Thomas Alt,§ Jérôme Pellaud,§ and Anna Seelig*,§

Institut für Medizinische Physik und Biophysik, Medizinische Fakultät Charité der Humboldt-Universität, Berlin, Germany, and Department of Biophysical Chemistry, Biocenter, University of Basel, Klingelbergstrasse 70, CH 4056 Basel, Switzerland

Received February 8, 1999; Revised Manuscript Received April 19, 1999

ABSTRACT: Transducin is a heterotrimer formed by a fatty acylated α-subunit and a farnesylated $\beta\gamma$-subunit. The role of these two covalent modifications and of adjacent hydrophobic and charged amino acid residues in reversible anchoring at disk model membranes is investigated at different pH values, salt concentrations, and lipid packing densities using the monolayer expansion technique and CD spectroscopy. The heterotrimer only binds if the acetylated α-subunit is transformed into its surface-active form by divalent cations. In the presence of salts the α(GDP)-subunit, the $\beta\gamma$-complex, and the heterotrimer bind to POPC monolayers at 30 mN/m, estimated to mimic the lateral packing density of disk membranes, with apparent binding constants of $K_{app} = (1.1 \pm 0.3) \times 10^6$ M^{-1} (reflecting the penetration of the fatty acyl chain together with approximately three adjacent hydrophobic amino acid residues), $K_{app} = (3.5 \pm 0.5) \times 10^6$ M^{-1} (reflecting the penetration of the farnesyl chain), and $K_{app} = (1.6 \pm 0.3) \times 10^6$ M^{-1} (reflecting a major contribution of the α(GDP)-subunit with only a minor contribution from the $\beta\gamma$-complex). The apparent binding constant of the α(GTP)-subunit is distinctly smaller than that of the α(GDP)-subunit. Binding to negatively charged POPC/POPG (75/25 mole/mole) monolayers is reinforced by 2−3 cationic residues for the $\beta\gamma$-complex. The α-subunit shows no electrostatic attraction and the heterotrimer shows even a slight electrostatic repulsion which becomes the dominating force in the absence of salts.

Heterotrimeric guanine nucleotide-binding proteins or G-proteins (G) act as universal transducers in membrane-bound signal transduction. Generally, the heterotrimer, composed of the α-subunit (G_α) and the undissociable $\beta\gamma$-subunit complex ($G_{\beta\gamma}$), couples to seven-helix transmembrane receptors at the cytoplasmic face of the plasma membrane. Receptors activated by specific chemical or physical stimuli, such as hormones or quanta of light, induce exchange of GTP for GDP on G_α and dissociation of G_α from $G_{\beta\gamma}$. Both G_αGTP and $G_{\beta\gamma}$ can interact with various effector molecules. The intrinsic GTP hydrolytic activity of G_α converts it back to the GDP-bound resting state, which reassociates with $G_{\beta\gamma}$.

Signal transduction in the retinal rod is one of the best-characterized G-protein-coupled signaling systems (for review, see ref *3*). The crystal structure of a modified heterotrimeric transducin, the G-protein coupling to rhodopsin (G_t), has recently been determined (*4*). The modified heterotrimeric complex consists of a $G_{t\alpha}/G_{i\alpha1}$[1] chimera, and an endo-Lys-C-proteolyzed $G_{t\beta\gamma}$. $G_{t\alpha}/G_{i\alpha1}$, expressed in *Escherichia coli* is missing the fatty acyl modification. $G_{t\beta}$ of the endo-Lys-C-proteolyzed $G_{t\beta\gamma}$ is intact, but the three C-terminal residues of $G_{t\gamma}$ and the farnesyl modification are missing. The present crystal structure includes residues 6−343 for $G_{t\alpha}/G_{i\alpha1}$, residues 2−340 for $G_{t\beta}$, and 8−66 for $G_{t\gamma}$.

The native α-subunit (39 kDa) of transducin is acylated at the N-terminal glycine via an amide linkage. The fatty acyl modification is heterogeneous, containing laurate (C12:0), unsaturated C14:2 and C14:1 fatty acids, and only 5% of myristate (C14:0) (*5*, *6*). Nevertheless we will refer to these hydrophobic modifications as myristate. The γ-subunit (8 kDa), tightly associated to the β-subunit (36 kDa) as $\beta\gamma$-complex ($G_{t\beta\gamma}$), is farnesylated (C_{15}) via a thioether bond and reversibly α-carboxyl methylated at the C-terminal cysteine residue (*7*).

The hydrophobic modifications have been shown to play a role in membrane targeting of G-proteins in general and may also affect protein−protein interactions (cf. ref *8*). In solution neither N-acylation of $G_{t\alpha}$GDP nor farnesylation of $G_{t\beta\gamma}$ seems to significantly contribute to the association of $G_{t\alpha}$ with $G_{t\beta\gamma}$ (*9*). Both $G_{\beta\gamma}$ (*9*, *10*) and G_αGDP (*9*, *11*) can interact separately with phospholipid membranes. In the absence of the hydrophobic modifications, membrane association of both G_α (*9*, *12*) and $G_{\beta\gamma}$ (*9*) is lost. G_αGDP will only associate with $G_{\beta\gamma}$ to form the heterotrimer if both subunits carry their hydrophobic modifications and if a lipid membrane or a detergent micelle acts as a matrix (*9*, *13*). Whether both hydrophobic modifications of G_t penetrate into

† This work was supported by the Deutsche Forschungsgemeinschaft (SFB 366) and the Fonds der Chemischen Industrie and by the Swiss National Science Foundation Grant 31.42058.9.

* Corresponding author. Fax: +41-61-267-2206. E-mail: seeliga@ubaclu.unibas.ch.

‡ Medizinische Fakultät Charité der Humboldt-Universität.

§ Biocenter, University of Basel.

[1] Abbreviations: G_t, transducin (heterotrimer); $G_{t\alpha}$, α-subunit; $G_{t\alpha}$-GTPγS, guanosine 5′O-(3-thio) triphosphate (GTPγS) containing $G_{t\alpha}$, $G_{t\beta\gamma}$, $\beta\gamma$-complex; POPC, 1-palmitoyl-2-oleoyl-*sn*-glycero-3-phosphocholine; POPG, 1-palmitoyl-2-oleoyl-*sn*-glycero-3-phosphoglycerol.

10.1021/bi990298+ CCC: $18.00
Published on Web 06/03/1999

the membrane (*9*) or whether only the myristoyl moiety penetrates, while the farnesyl moiety interacts with the α-subunit (*14*), is not yet fully clarified.

In addition to hydrophobic interactions, electrostatic interactions (*14*) were shown to play a role in binding of $G_{t\beta\gamma}$ to negatively charged membranes. In this context the early observation that the heterotrimer in its inactive, GDP-binding form can be easily extracted from disk membranes at low ionic strength (*15*) suggests a special role of ions for disk membrane binding which is not yet understood.

Disk membranes are unusual in their high content of lipids with polyunsaturated acyl chains in the *sn*-2 position. These lipids exhibit a relatively large cross-sectional area, and as a consequence, their lateral packing density is lower than that of lipids with monounsaturated acyl chains in the *sn*-2 position. The latter was determined previously as 32 ± 1 mN/m (*16*) in the absence and as 35 ± 1 mN/m in the presence of cholesterol (*17*). In contrast to cholesterol, which strongly increases acyl chain ordering in membranes, transmembrane proteins reduce it, but only to a small extent (∼10%) (for review, see refs *18*, *19*). To a first approximation the lateral packing density in the presence or absence of transmembrane proteins can therefore be assumed to be similar. On the basis of X-ray and ^{2}H NMR measurements (*20*), the lateral packing density in disk membranes at the tip of the rod outer segments is estimated as 30 mN/m. The fact that G-protein activation increases progressively with decreasing levels of cholesterol and increasing levels of acyl chain unsaturation (*21*) points to an important role of the lipid packing density. The packing density of membranes may also change in the course of an activation cycle as a result of phospholipase action (cf. ref *22*).

Proper membrane association of molecules involved in G-protein-coupled signal transduction is thought to be a decisive factor in terms of precision and fidelity of signal transduction (*23*, *24*). Unraveling the disk membrane−transducin interaction on a molecular level may therefore be a prerequisite for understanding how the interaction of transducin with photoactivated rhodopsin is initiated (cf., e.g., ref *25*).

The aim of the present investigation is to provide for the first time quantitative membrane-binding data for transducin and its subunits. Since pH and ionic composition may change in the course of an activation cycle, binding measurements are performed at different pH values and different ion concentrations. As model systems we use small unilamellar vesicles and lipid monolayers which can be easily varied in their lateral packing density and thus allow the simulation of the potential surface pressure variations in disk membranes. Model membranes are composed either of electrically neutral 1-palmitoyl-2-oleoyl-*sn*-glycero-3-phosphocholine (POPC) or of a mixture of POPC and negatively charged 1-palmitoyl-2-oleoyl-*sn*-glycero-3-phosphoglycerol (POPG) (75/25 mole/mole), which mimics the negative surface potential of the cytoplasmic side of disk membranes (cf. ref *26*). The following experiments are conducted: (i) The cross-section of the membrane penetrating moieties of $G_{t\alpha}$, $G_{t\beta\gamma}$, and G_t is determined by means of monolayer expansion measurements at constant surface pressure. (ii) Membrane-binding constants of $G_{t\alpha}$GDP, $G_{t\alpha}$GTP, $G_{t\beta\gamma}$, and G_t are estimated by measuring binding isotherms for electrically neutral and negatively charged monolayers at both 30 and 32 mN/m. The binding isotherms are analyzed in terms of hydrophobic and electrostatic interactions. (iii) The secondary structure of transducin in solution and bound to lipid vesicles is investigated by means of circular dichroism (CD) spectroscopy and is then compared to the crystal structure (*4*), to test experimentally whether the crystal structure can be used as an approximate model for the membrane-bound protein as suggested earlier (*25*). This combined approach provides the molecular determinants responsible for reversible membrane anchoring of transducin and allows one to propose a model for the membrane-binding region, which is essentially missing in the crystal structure.

MATERIALS AND METHODS

Purification of Transducin. Bovine G_t was purified as described by Heck and Hofmann (*27*). Purification of G_t subunits was carried out essentially as described by Yamazaki et al. (*28*) on a blue sepharose column (HiTrap Blue, 1 mL, Pharmacia). Aliquots were stored in 10 mM Hepes (pH 7.5) containing 100 mM NaCl, 5 mM $MgCl_2$, and 1mM DTT at −80 °C.

$G_{t\beta\gamma}$ concentration was determined by the method of Bradford (*29*) using bovine serum albumin as the standard. Active G_t and $G_{t\alpha}$ concentrations were determined by fluorimetric titration using GTPγS (*30*).

Buffers. For monolayer-binding measurements 10 mM Hepes (pH 7.0−8.0) or 10 mM MES (pH 5.5−6.5), containing 1 mM $MgCl_2$, 100 mM NaCl, and 1 mM DTT, was used if not otherwise specified. For CD measurements 10 mM Tris (neutral and basic pH) or MES was used. Concentrations of monovalent and divalent salts were identical to that above if not otherwise mentioned, but NaCl which absorbs strongly at low wavelength (λ < 200 nm) was replaced by NaF. This exchange had, however, no influence on the spectral shape of the protein. When present with 1 mM Mg^{2+}, NaF transforms G_t into an at least partially active conformation (ref *31*; see below).

Lipids and Lipid Vesicle Preparation. POPC and POPG were purchased from Avanti Polar Lipids (Birmingham, Alabama) and were used without further purification. Lipid vesicles were prepared as described earlier (*32*).

Circular Dichroism Measurements. Circular dichroism (CD) spectra were measured with a Jasco J720 spectropolarimeter at ambient temperature as described earlyer (*33*). Results were plotted as mean residue ellipticity, Θ, in units of deg cm^2 dmol^{-1}. Estimations of the percentage of secondary structures were obtained from a computer simulation based on the reference spectra of Yang et al. (*34*). CD spectroscopy was used to ensure that the secondary structure of the protein was essentially unchanged under the conditions of these measurements.

Monolayer Measurements. A round Teflon trough designed by Fromherz (*35*) (type RCM 2-T, Mayer Feintechnik, Göttingen, Germany) with a total area of 362 cm^2, divided into eight compartments was used. To keep humidity constant, we filled compartments, which were not used for measurements, with water and covered the trough with a Plexiglas hood. The surface pressure, $\pi = \gamma_0 - \gamma$, where γ_0 is the surface tension of the pure buffer and γ the surface tension of the peptide solution, was monitored by means of a Whatman No. 1 filter paper, connected to a Wilhelmy

balance. Measurements were performed at ambient temperature 23 ± 1 °C.

For penetration experiments generally two compartments of the trough were used, containing together 40 mL of solution. The monolayer was formed by depositing a drop of lipid dissolved in hexane/ethanol (9:1, v/v) on the buffer surface between a fixed and a movable barrier and was then left to stabilize for about 15 min. The initial area, A, of the lipid monolayer was typically around 50 cm^2 and contained n_L lipid molecules. Protein dissolved in buffer (5−15 μM) was injected with a Hamilton syringe into the buffer subphase which was stirred continuously by a magnetic stirring bar. During equilibration time the surface pressure, π, was kept constant by means of an electronic feedback system. The penetration of n_P protein molecules with an penetration area, A_P, into the monolayer thus gave rise to an area expansion, ΔA. The mole fraction of protein in the monolayer is defined as $X_b = n_P/n_L$, and can be evaluated from the relative area increase, $\Delta A/A$, provided that A_L and A_P are known (see below) (*16*).

$$X_b = n_P/n_L = (\Delta A/A)(A_L/A_P) \quad (1)$$

Evaluation of Partition Coefficients. The monolayer expansion method provides the possibility to measure binding isotherms in the nanomolar concentration range. At these low concentrations the penetration of the protein into the lipid monolayer can be described by a simple partition equilibrium[2]

$$X_b = K_{app}C_{eq} \quad (2)$$

where K_{app} is the partition coefficient or apparent binding constant and C_{eq} the equilibrium concentration of the protein in solution. The latter is calculated according to

$$C_{eq} = C_{tot} - (C_b + C_{ads}) \quad (3)$$

where C_{tot} is the total concentration of protein, C_b is the concentration of protein bound to the lipid monolayer (*32*), and C_{ads} is the concentration adsorbed to the Teflon trough. Adsorption to the Teflon surface was found to be distinctly smaller than that to the lipid monolayer. For simplicity we used a constant value, $C_{ads} = 2$ nM for G_t as well as for its subunits.

K_{app} was determined from a Scatchard plot at low concentrations (nM). This simple model was found to be appropriate previously for hisactophilin binding to lipid monolayers (*33*).

However, at high concentrations a saturation behavior is observed, indicating a complete coverage of the available lipid monolayer with the protein. The experimental $\Delta A/A$ vs C_{eq} curves (Figure 3) were therefore fitted with a Langmuir adsorption isotherm of the form

$$\Delta A/A = (A_P/A_L)(K_{app}C_{eq})/(1 + (nC_{eq}K_{app})) \quad (4)$$

where K_{app} is the apparent binding constant (cf. above) and n is the number of lipids covered by one protein molecule.

[2] Effects due to steric hindrance of large protein molecules (*1*) which play a role in the μM concentration range can be neglected at these low concentrations.

Measurement of the Penetration Area of the Protein. To penetrate into a lipid monolayer with a lateral pressure, π, a protein molecule has to perform the work $\Delta W = \pi A_P$, where the penetration area, A_P, is the area which the molecule occupies in the lipid monolayer. The free energy of penetration will therefore vary with the monolayer surface pressure, π. According to Boguslavsky et al. (*36*) the variation of the partition coefficient, K_{app}, with the surface pressure is given by

$$K_{app} = K_0 e^{-\pi A_P/kT} \quad (5)$$

Combining eqs 1 and 5 yields the surface pressure dependence of the relative area increase, $\Delta A/A$, at constant C_{eq} under the assumption of a constant penetration area, A_P, and a constant lipid area, $A_L$in the following:

$$\Delta A/A = (A_P/A_L)K_0C_{eq}e^{-\pi A_P/kT} \approx (\text{const})e^{-\pi A_P/kT} \quad (6)$$

The penetration area, A_P, was determined from the slope of the ln($\Delta A/A$) vs π curve. In the case of biphasic ln($\Delta A/A$) vs π curves the two areas, A_{P1} and A_{P2}, are assumed to be constant for the given surface pressure interval. The assumption of constant area can be made to a first approximation since A_L and A_P change by at most 15% in a given surface pressure interval.

Error Determination. For monolayer insertion measurements each data point corresponds to an experiment performed with a fresh lipid monolayer. For one $\Delta A/A$ vs π or $\Delta A/A$ vs C_{eq} curve, protein from different preparations was used (exceptions are mentioned). The scatter thus reflects the error in protein concentration as well as in monolayer manipulation. The errors in A_p and K_{app} were determined from the standard deviations of the measured curves.

Molecular Modeling. Structural data (*4*) were obtained from the SBX Brookhaven data bank.

RESULTS

Penetration of $G_{t\alpha}$, $G_{t\beta\gamma}$, and G_t into Lipid Monolayers as a Function of the Surface Pressure. A lipid monolayer with an area, A, was spread on buffer containing 1 mM $MgCl_2$ and 100 mM NaCl and was set to a desired surface pressure (π), which was kept constant during the penetration experiment. The surface pressure of the lipid monolayer was always distinctly higher than the surface pressure of the protein in solution. The protein was injected into the subphase to a final concentration of $C_{tot} = 20$ nM and gave rise to an area increase (ΔA) due to penetration into the lipid layer. Monolayers in the presence of $G_{t\alpha}$, $G_{t\beta\gamma}$, and G_t were extremely stable. The equilibration times were of 2−3 h. The rate-limiting step is the diffusion of the protein to the monolayer surface. Figure 1 summarizes the penetration measurements of $G_{t\alpha}$, $G_{t\beta\gamma}$, and G_t into POPC/POPG (75/25 mole/mole) monolayers as a function of surface pressure.

For $G_{t\alpha}$GDP (Figure 1A) the semilogarithmic plot of $\Delta A/A$ vs π at pH 7.5 is linear in the surface pressure range of 23−29 mN/m. In the small surface pressure interval of $\pi \cong 29$−31 mN/m, a steep sigmoidal decrease of ln($\Delta A/A$) is observed. From the linear slope of the ln($\Delta A/A$) vs π curve

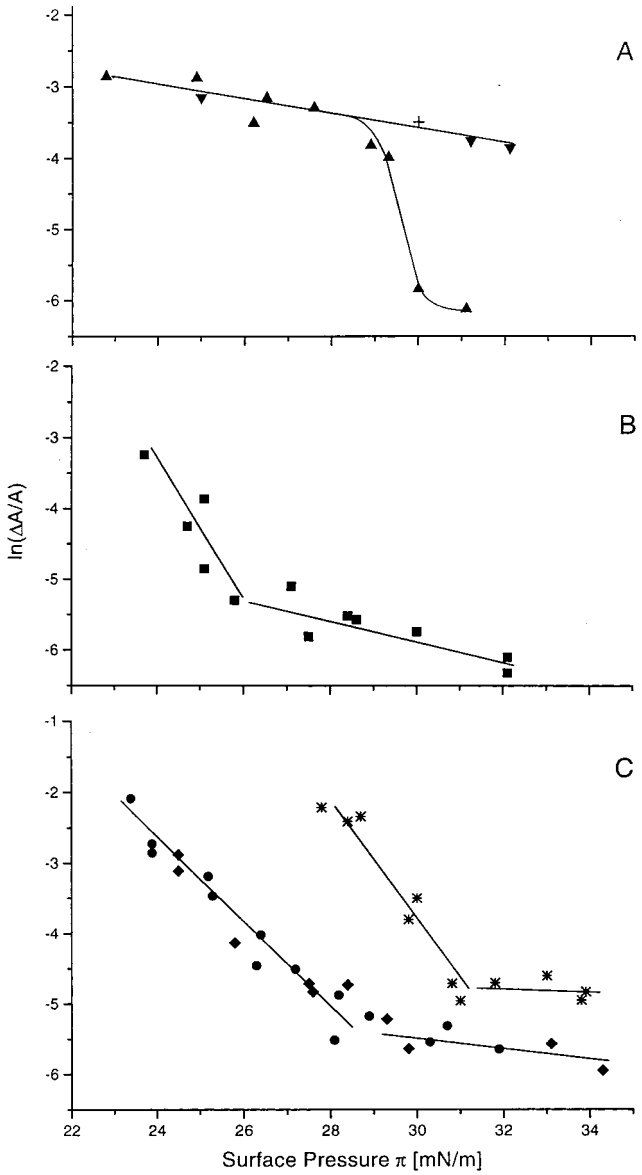

FIGURE 1: Relative area increase, $\Delta A/A$, due to protein ($C_{tot} = 20$ nM) penetration into POPC/POPG (75/25 mole/mole) monolayers as a function of the monolayer surface pressure, π: (A) $G_{t\alpha}$GDP at pH 7.5 (▲) and pH 5.5 (+) and $G_{t\alpha}$GTPγS at pH 5.5 (▼); (B) $G_{t\beta\gamma}$ at pH 7.5 (■); (C) G_t at pH 7.0 (●), pH 8.0 (◆), and pH 5.5 (*). Each experimental point represents a new lipid monolayer with a preset surface pressure, π, kept constant during the penetration experiment.

(23−29 mN/m) the cross-sectional area of $G_{t\alpha}$GDP in the lipid monolayer is determined according to eq 6 as $A_P = 65 \pm 10$ Å^2.

Penetration of $G_{t\alpha}$GTPγS into POPC/POPG (75/25 mole/mole) monolayers at pH 7.5 (not shown) is practically identical to that of $G_{t\alpha}$GDP at low surface pressure. However, the sigmoidal drop of the ln($\Delta A/A$) vs π curve occurs already in a lower surface pressure range (26−27 mN/m). At pH 5.5 the ln($\Delta A/A$) vs π curve of $G_{t\alpha}$GTPγS (Figure 1A) is superimposable to that of $G_{t\alpha}$GTPγS and $G_{t\alpha}$GDP (pH 7.5) at low surface pressure but remains linear in the whole surface pressure range measured. The same seems to be true for $G_{t\alpha}$GDP at pH 5.5.

For $G_{t\beta\gamma}$ (Figure 1B) the ln($\Delta A/A$) vs π plot shows a biphasic behavior. At low surface pressures (23−28 mN/m) the relative area increase varies strongly with π, while at high surface pressures ($\pi > 30$ mN/m) the variation is small. The penetration areas derived from the two different slopes of the curve (cf. Methods) are $A_{P1} = 280 \pm 20$ Å^2 and $A_{P2} = 80 \pm 20$ Å^2 in the low and the high surface pressure range, respectively.

Figure 1C shows the ln($\Delta A/A$) vs π plot for G_t measured at pH 7.0, 8.0, and 5.5. The curves at pH 7.0 and 8.0 are identical within experimental error and exhibit a biphasic behavior similar to that of $G_{t\beta\gamma}$. The corresponding penetration areas are $A_{P1} = 264 \pm 20$ Å^2 and $A_{P2} = 60 \pm 10$ Å^2. At pH 5.5 a similar biphasic behavior is observed, but the relative area increase is distinctly higher in the whole surface pressure range measured. The penetration areas are $A_{P1} = 300 \pm 20$ Å^2 and $A_{P2} = 58 \pm 10$ Å^2.

The ln($\Delta A/A$) vs π curve of G_t for electrically neutral POPC monolayers (not shown) is comparable to that of $G_{t\alpha}$ for POPC/POPG monolayers at low surface pressure but remains linear in the surface pressure range 25−32 mN/m. From the slope of the linear curve the penetration area, $A_P = 73 \pm 20$ Å^2 is determined.

Binding Isotherms of $G_{t\alpha}$, $G_{t\beta\gamma}$, and G_t. Protein binding to POPC/POPG (75/25 mole/mole) and POPC monolayers was measured by monitoring the relative area increase, $\Delta A/A$, as a function of the equilibrium concentration, C_{eq}. The $\Delta A/A$ vs C_{eq} curves can be transformed into true binding isotherms according to eq 1 since the area of the lipids, A_L (*37*), and the penetration area of the proteins, A_P, at membrane packing densities are known (cf. Table1). Binding isotherms were measured both at 30 and at 32 mN/m. Typical binding isotherms of $G_{t\alpha}$GDP, $G_{t\beta\gamma}$, and G_t measured for POPC/POPG (75/25 mole/mole) and POPC monolayers at 30 mN/m (pH 7.5) are displayed in Figure 2. Binding isotherms were also measured at pH 5.5 both at 30 and 32 mN/m. Partition coefficients were determined according to eqs 1 and 2 and are summarized in Table 1.

At high concentrations of G_t and its subunits, a saturation behavior is observed indicating a complete coverage of the available lipid monolayer with the protein. For lipid monolayers at 30 mN/m, in the absence of electrostatic attraction between proteins and the monolayer surface, the number of lipids covered by one protein molecule was evaluated according to eq 4 as $n = 15 \pm 4$ for G_t (POPC/POPG) as well as for $G_{t\alpha}$ (POPC/POPG) and $G_{t\beta\gamma}$ (POPC). This suggests an area requirement of 1020 ± 270 Å^2 per protein molecule.[3]

The Influence of Ionic Strength and pH on Protein Penetration. A POPC/POPG (75/25 mole/mole) monolayer was spread on buffer solution at pH 7.5 in the absence of $MgCl_2$ and NaCl at a surface pressure of 25 mN/m. No area increase was observed after injection of $G_{t\alpha}$ and G_t into the subphase. Penetration was only triggered by injecting $MgCl_2$. Increasing the concentration of $MgCl_2$ lead to increasing penetration of the proteins as exemplified for G_t in Figure 3A. $CaCl_2$ had almost the same effect. However, NaCl at the same concentration was about twenty times less effective.

[3] For negatively charged monolayers (POPC/POPG) the number of lipid molecules covered by one $G_{t\beta\gamma}$ molecule appears to be larger ($n = 32 \pm 2.4$) than for neutral monolayers. However, this may be an artifact. Due to electrostatic attraction the concentration of $G_{t\beta\gamma}$ at the negatively charged monolayer surface is high (cf. discussion). At elevated bulk concentrations binding may therefore be reduced as a result of steric hindrance.

Table 1: Parameters for Transducin and Its Subunits Derived from Monolayer-Binding Experiments[a]

	pH	π [mN/m]	$G_{t\alpha}GDP$	$G_{t\alpha}GTP_\gamma S$	$G_{t\beta\gamma}$	G_t
A_{p1} (PC/PG) [Å^2]	7.5	<30	65 ± 10	65	280 ± 20	264 ± 20
A_{p2} (PC/PG) [Å^2]	7.5	>30	65 ± 10	nm	80 ± 20	60 ± 10
A_p (PC) [Å^2]	7.5	<30	nd	nd	nd	73 ± 20
A_{p1} (PC/PG) [Å^2]	5.5	<30	65 ± 10	65	nd	300 ± 20
A_{p2} (PC/PG) [Å^2]	5.5	>30	65 ± 10	65	nd	58 ± 10
K_{app} (PC/PG) [M^{-1}]	7.5	32	nd	nd	nd	(8.4 ± 2) 10^4
K_{app} (PC) [M^{-1}]	7.5	32	(4.9 ± 1) 10^4	nd	(1.1 ± 0.4) 10^5	(4.8 ± 1) 10^5
K_{app} (PC/PG)/K_{app} (PC)	7.5	32	nd	nd	nd	0.2
K_{app} (PC/PG) [M^{-1}]	7.5	30	(1.1 ± 0.4) 10^6	$<1 \times 10^5$	(3.5 ± 1.0) 10^6	(1.6 ± 0.4) 10^6
K_{app} (PC) [M^{-1}]	7.5	30	∼(1.1 ± 0.4) 10^6	nd	(1.2 ± 0.3) 10^5	(2.5 ± 0.6) 10^6
K_{app} (PC/PG)/K_{app} (PC)	7.5	30	1	nd	29	0.6
charge, z_{eff}	7.5	30	∼0	nd	2.7+	0.5−
amino acid residues	7.5	30	E8, E9, K10 (H11)	nd	K61, K65, K68	E8, E9, K10 (H11)
K_{app} (PC/PG) [M^{-1}]	5.5	32	nd	nd	nd	(9.5 ± 3) 10^6
K_{app} (PC/PG) [M^{-1}]	5.5	30	(1.0 ± 0.5) 10^7	nd	$<3.5 \times 10^6$	(5.0 ± 0.7) 10^7
influence of $MgCl_2$	7.5	25	strong	nd	weak	strong

[a] nm: not measurable at a protein concentration of 20 nM. nd: not determined.

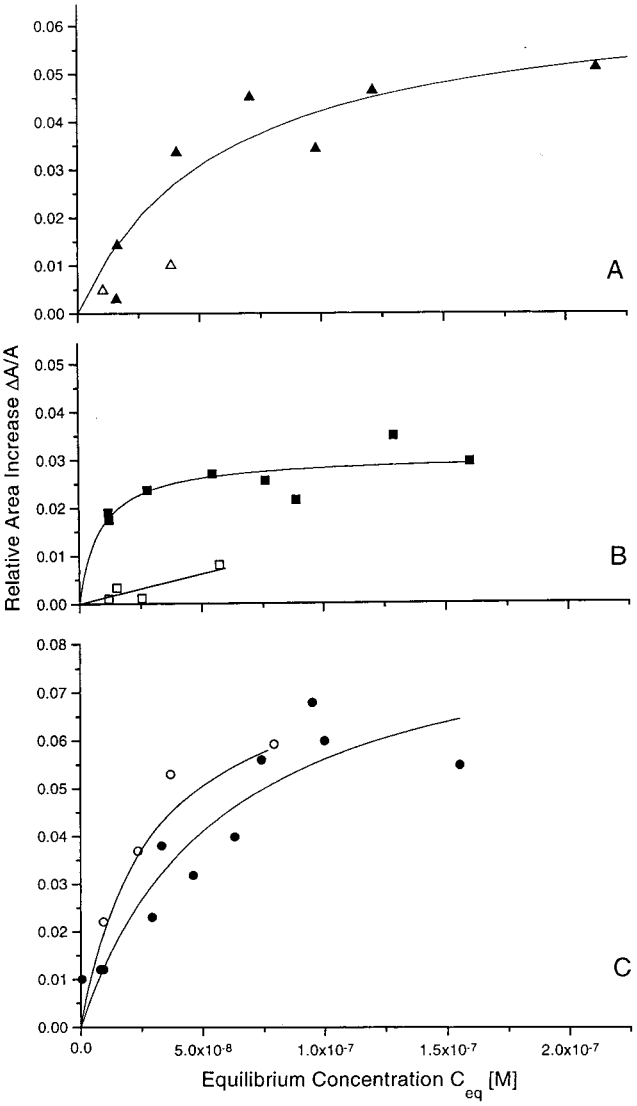

FIGURE 2: Relative area increase, $\Delta A/A$, of POPC/POPG (75/25 mole/mole) (solid symbols) and POPC (open symbols) monolayers at π = 30 mN/m, respectively, as a function of the equilibrium concentration, C_{eq} at pH 7.5: (A) $G_{t\alpha}GDP$ (▲, △); (B) $G_{t\beta\gamma}$ (■, □); (C) G_t (●, ○). The experimental points are fit to a Langmuir adsorption isotherm. The parameters used for fitting are the apparent partition coefficients, K_{app}, determined independently at low concentrations and the number of lipid molecules covered by one protein molecule, *n*.

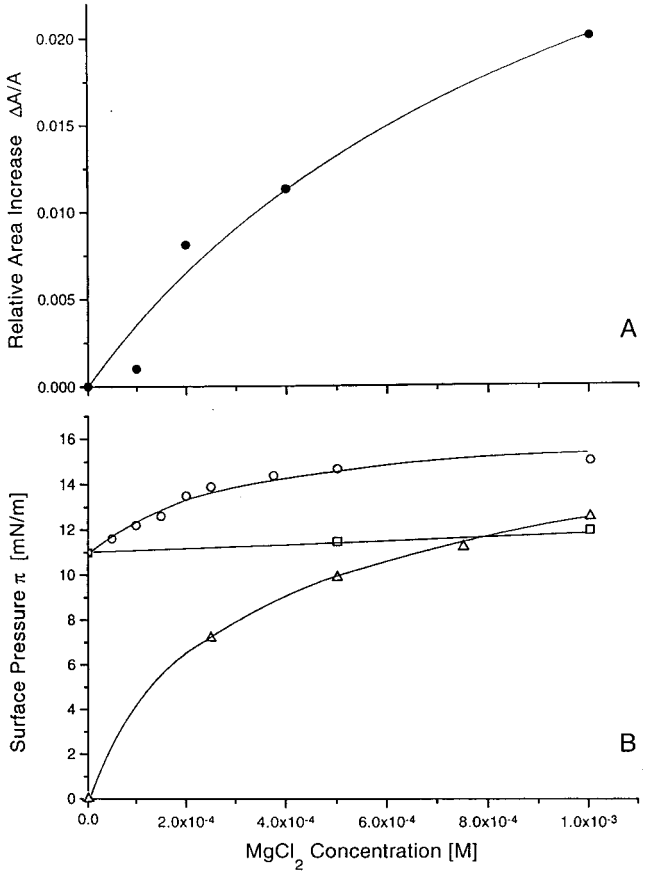

FIGURE 3: (A) G_t (C_{tot} = 20 nM) penetration into POPC/POPG (75/25 mole/mole) monolayers at 25 mN/m (10 mM buffer pH 7.5, no NaCl) as a function of the $MgCl_2$ concentration. (B) Surface pressure, π, of $G_{t\alpha}$ (△), $G_{t\beta\gamma}$ (□), and G_t (○) in solution (same buffer, no lipids, C_{tot} = 20 nM) as a function of the $MgCl_2$ concentration. Experimental points are fit to a Langmuir adsorption isotherm (A) and to the Szyszkowski equation (cf. ref *51*) (B).

Penetration of $G_{t\beta\gamma}$ into the lipid monolayer was also observed in the absence of salts, however, to a slightly lower extent. For comparison Figure 3B displays the surface pressure of G_t and its subunits in buffer solution (in the absence of lipids) as a function of the $MgCl_2$ concentration. $G_{t\alpha}$ shows a strong, $G_{t\beta\gamma}$ a weak, and G_t an intermediate surface activity increase as a function of the $MgCl_2$ concentration. In contrast to $G_{t\beta\gamma}$ and G_t, $G_{t\alpha}$ is not surface-active

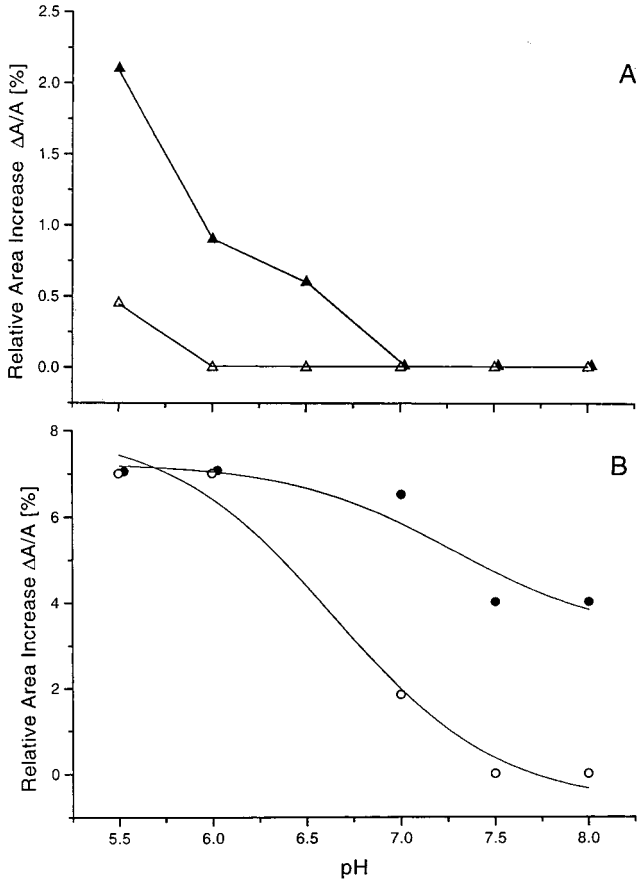

FIGURE 4: (A) Relative area increase, $\Delta A/A$, due to protein penetration into POPC/POPG (75/25 mole/mole) monolayers at 32 mN/m as a function of pH in the absence (open symbols) and presence (solid symbols) of salts (100 mM NaCl, 1 mM $MgCl_2$). (A) $G_{t\alpha}$ (20 nM) (▲, △), solid lines drawn to guide the eye. (B) G_t (49.5 nM) (●, ○), solid lines represent titration curves. (Fischer et al., 1998)

in the absence of salts, not even at high protein concentrations (200 nM).

The influence of pH on the penetration of $G_{t\alpha}$GDP into POPC/POPG (75/25 mole/mole) monolayers at 32 mN/m was investigated in the presence and absence of $MgCl_2$ and NaCl (Figure 4A). In the presence of salts, no penetration is observed in the range of pH 7.0−8.0. However, with decreasing pH penetration increases. In the absence of salts penetration starts only below pH 6.0.

The penetration behavior of G_t under similar conditions is shown in Figure 4B. In the absence of salts no penetration is observed in the range of pH 7.5−8.0, whereas at acidic pH penetration also occurs in the absence of salts. Penetration in the presence of salts is again higher. In the case of G_t the lack of cations can be compensated by protons.

To estimate whether the increase in membrane penetration observed for G_t is due to an increase in surface activity of the protein in solution or to a change in the charge of the membrane contact region (cf. discussion), we measured the surface activity of G_t (20 nM) in the presence of salts as a function of pH in the range 5.5−9.5 (not shown). A surface pressure minimum was observed around pH 7.5 ($\pi = 15.5 \pm 0.5$ mN/m). It was ∼20% lower than the maxima at pH 5.5 and 8.0, respectively. The surface pressure minimum corresponds to the solubility maximum of the protein and is due to a maximum number of ionized residues at pH 7.5.

The Secondary Structure of G_t and Its Subunits in Solution and in the Presence of Lipid Vesicles as Monitored by Means of CD Spectroscopy. The CD spectra of $G_{t\alpha}$, $G_{t\beta\gamma}$, and G_t, at pH 7.5 in buffer solution (no salts) are shown in Figure 5A−C. For comparison the three spectra were simulated with the structural data obtained by X-ray analysis for the inactive GDP-bound form[4] (*4*) by using the reference CD spectra of Yang et al. (*34*). The following percentages of α-helix, β-sheet, and β-turns plus random coil were used: 49%, 12%, and 37% for $G_{t\alpha}$; 14%, 39%, and 47% for $G_{t\beta\gamma}$; and 30%, 27%, and 47% for G_t. Figure 5A−C reveals a good agreement between the simulated and the experimental spectra. The shape of the spectra did not change in the pH range 7.5−5.5. The secondary structure thus appears to be similar in solution and in the crystal.

A further decrease of the pH leads to a small ellipticity increase for G_t around 217 nm (not shown). The maximum increase in ellipticity (12%) is reached at pH 4.1. The apparent ionization constant derived from this titration is $pK_a = 4.7$ and thus suggests that the ellipticity increase is due to glutamic acid protonation (J. Pellaud, M. Heck, K. P. Hofmann, and A. Seelig, manuscript in preparation). Even at pH 2.5 no increase in random coil conformation is observed. This high acid stability of G_t is unusual. Many other proteins, for example, hisactophilins, denature at pH < 4 (*33*).

In the presence of salts (1 mM $MgCl_2$ and 100 mM NaF), which are required for membrane penetration, the spectra of $G_{t\alpha}$, $G_{t\beta\gamma}$, and G_t at pH 7.5 show the same shape as in the absence of salts, but their intensity is lower as exemplified for G_t (Figure 5D). The intensity reduction results from the formation of small aggregates or micelles and is due to optical flattening (*38*). At pH 5.5 the spectra of G_t (Figure 5D) and $G_{t\alpha}$, but not of $G_{t\beta\gamma}$ (not shown) exhibit a further intensity reduction, especially at low wavelength which is typical for light-scattering effects and suggests the formation of larger aggregates. A further acidification leads to increasing protein aggregation.

Addition of small unilamellar POPC/POPG (75/25 mole/mole) vesicles in the presence or absence of 1 mM $MgCl_2$ and 100 mM NaF induces practically no spectral change for $G_{t\alpha}$, $G_{t\beta\gamma}$ (not shown), and G_t (Figure 5D) at pH 7.5. However, at pH 5.5 the light-scattering effects observed for $G_{t\alpha}$ and G_t in solution disappear upon addition of lipid vesicles, and the spectra become superimposable to those measured at pH 7.5 (for G_t, spectra 1−4 in Figure 5D). This is consistent with aggregate dissociation upon protein binding to lipid vesicles.

DISCUSSION

Binding of transducin and its subunits to disk membrane mimicking systems is analyzed. The information gained from penetration areas and from hydrophobic and electrostatic binding energies will in the following be discussed in terms of molecular moieties involved. It will be shown that the region of contact between the proteins and the lipid membrane is small and comprises the elements missing in the crystal structure. Together with the crystal structure (*4*)

[4] The inactive form is similar in its secondary structure to the active form (*2*).

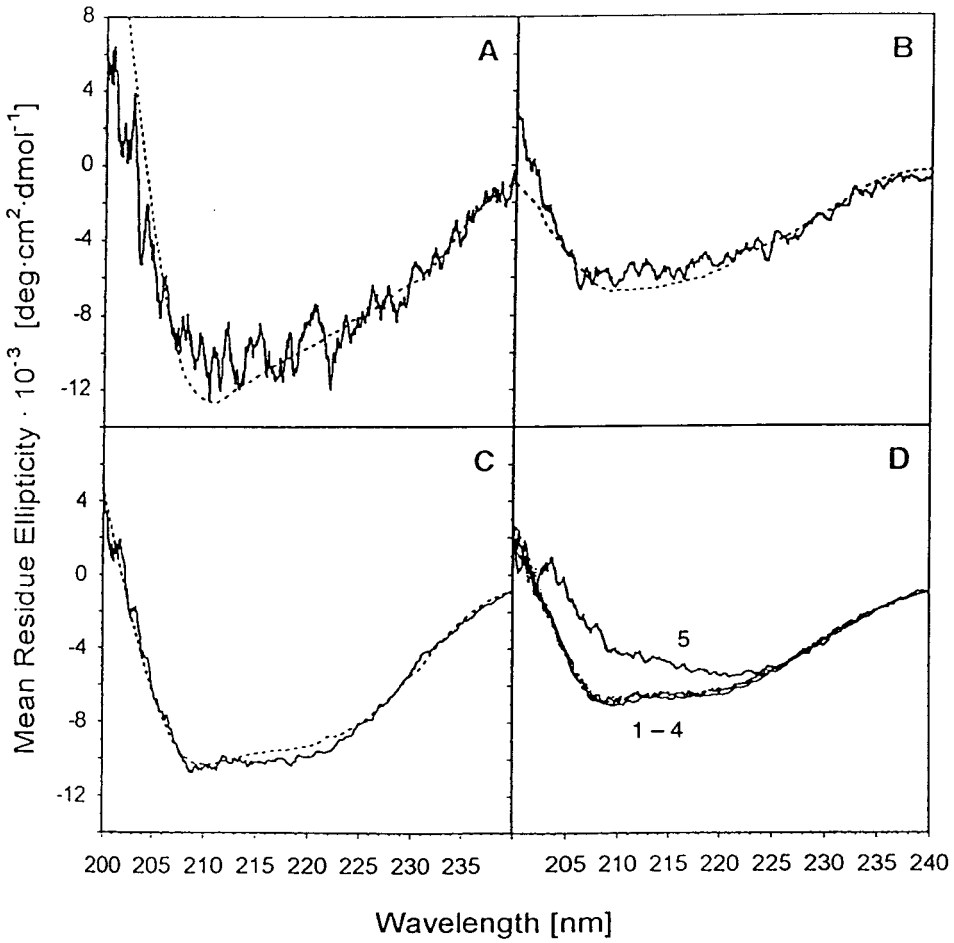

FIGURE 5: CD spectra of $G_{t\alpha}$ (0.9 μM) (A), $G_{t\beta\gamma}$ (2.0 μM) (B), and G_t (2.75 μM) (C), measured in 10 mM buffer at pH 7.5 (without additional salts). Dotted lines represent the spectra simulated on the basis of the crystal structure (*4*) using the reference spectra of Yang et al. (1986). (D) CD spectra of G_t (4 μM) measured in 10 mM buffer at pH 7.5, containing 100 mM NaF and 1 mM $MgCl_2$, in the absence and presence of POPC/POPG (75/25 mole/mole) vesicles (0, 0.1, 0.2, 0.4 mM) (1−4) and at pH 5.5 (4.1 μM) in the absence of lipid vesicles (5).

shown to be essentially preserved at the membrane surface, a molecular model of the membrane recognition region of transducin and its subunits will be proposed.

$G_{t\alpha}$ and $G_{t\beta\gamma}$ Are Anchored at the Membrane with Their Myristoyl and Farnesyl Extensions, Respectively. Monolayer expansion measurements allow the determination of the extent of protein penetration into the lipid layer. The penetration area of $G_{t\beta\gamma}$ measured for POPC/POPG (75/25) monolayers at a lateral packing density corresponding to that of lipid bilayers (*16*) is $A_P = 80 \pm 20$ Å^2. That of $G_{t\alpha}$ could only be measured at $\pi < 30$ mN/m and is $A_P = 65 \pm 10$ Å^2. It was assumed to be similar at higher surface pressures. The penetration areas of the two subunits are thus larger than those of the myristic acyl chain (21 ± 2 Å^2) and the farnesyl chain (33 ± 2 Å^2) in their extended conformation as determined by molecular modeling and therefore suggest some contributions from amino acids adjacent to the hydrophobic moieties.

The hydrophobic binding constants of the two subunits were determined by measuring the area increase due to protein penetration into electrically neutral monolayers at the lateral packing densities of both 32 and 30 mN/m. At low protein concentrations penetration of the hydrophobic regions into the lipid monolayers is a simple partitioning process. For neutral POPC monolayers at 32 mN/m the partition coefficient of $G_{t\alpha}$ is $K_{app} = (4.9 \pm 1) \times 10^4$ M^{-1}. This is somewhat higher than the partition coefficient of small myristoylated model peptides binding to electrically neutral lipid bilayers ($K = 1 \times 10^4$ M^{-1}) (*39*) and distinctly larger than the partition coefficient of model acetylated proteins (*40*). For $G_{t\beta\gamma}$ the partition coefficient is $K_{app} = 1.1 \times 10^5$ M^{-1}, which is close to that of a farnesyldiphosphate ($K = 1.2 \times 10^5$ M^{-1}) (*41*). It can thus be concluded that the interaction of each of the two subunits with neutral membranes is essentially due to the penetration of the hydrophobic extensions, with a small possible contribution from hydrophobic amino acid residues which is in agreement with conclusions drawn from penetration areas.

G_t Anchoring Is Due to $G_{t\alpha}$ with a Small Contribution of $G_{t\beta\gamma}$. The penetration area of G_t for POPC monolayers is $A_P = 73 \pm 20$ Å^2, independent of the lateral packing density (25−32 mN/m) which is in reasonable agreement with the penetration area, $A_P = 60 \pm 10$ Å^2, determined for POPC/POPG (75/25) monolayers at $\pi > 30$ mN/m. It is thus not the sum of the penetration areas of the two subunits, but rather corresponds to that of a single subunit. A penetration area of 60 ± 10 Å^2 is, however, still large enough to accommodate a myristoyl chain and a farnesyl chain in a extended conformation. Further information is therefore required to obtain an unambiguous answer.

The partition coefficient of G_t for neutral POPC monolayers at 32 mN/m is $K_{app} = (4.8 \pm 1) \times 10^5$ M^{-1}. This is

larger than the sum of the binding constants of $G_{t\alpha}$ and $G_{t\beta\gamma}$ (Table 1), but it is by far not as large as the product of the two binding constants ($\sim 10^9$ M^{-1}) which is expected for a synergistic interaction between the two hydrophobic modifications.

At 30 mN/m the cooperativity is even lower. A decrease in the lateral packing density of the POPC monolayer from 32 to 30 mN/m leads to an increase in the hydrophobic binding constant of $G_{t\alpha}$ by more than an order of magnitude. This could be due to a deeper penetration of the myristoyl moiety, most probably together with some adjacent hydrophobic amino acid residues (-Gly^2-Ala^3-Gly^4-Ala^5-Ser^6-Ala^7-). The number of amino acids involved can be roughly estimated from the difference in binding enthalpies at 30 and 32 mN/m ($\Delta G = -1.8$ kcal/mol). Assuming a contribution of $\Delta G = -0.6$ kcal/mol per hydrophobic amino acid side chain (*42*), three hydrophobic amino acid residues may be involved in anchoring $G_{t\alpha}$ at 30 mN/m.

The low synergistic interaction between the two hydrophobic modifications may be explained by different models: (i) The acyl and the farnesyl extension of the heterotrimer might penetrate in tight association. Considering the two extensions as bars, to a first approximation, each side contributes a factor $\sqrt[4]{K_{app}}$ to the binding constant. In a tight association the hydrophobic contributions of the hidden sides are lost. The partition coefficient of the myristoyl-farnesyl complex estimated on this basis using the partition coefficient of the acyl (*39*) and farnesyl extension (*41*), respectively, is $K_{app} \sim 5.6 \times 10^6$ M^{-1}. This is still higher by an order of magnitude than the measured binding constant. (ii) Only the myristoyl extension could penetrate as suggested earlier by Matsuda et al. (*14*). At first sight this model is in broad agreement with the experimental results: $G_{t\alpha}$ and G_t share similar hydrophobic binding constants at 30 mN/m, they both lack electrostatic attraction to negatively charged membranes, and their binding is strongly modulated by divalent cations and pH in contrast to that of $G_{t\beta\gamma}$ (cf. below). However, a closer look at the experimental details of the pH dependence of $G_{t\alpha}$ and G_t insertion (Figures 4) points to a more complex mechanism. On a thermodynamic basis the results could be best explained by a partial insertion of the farnesyl moiety or by a contribution of the α-carboxymethyl group of the C-terminal Cys^{71}.

Binding of $G_{t\beta\gamma}$ to Negatively Charged Lipids Is Reinforced by an Electrostatic Contribution, but Not That of $G_{t\alpha}$ and G_t. In the case of $G_{t\alpha}$ the apparent binding constant (K_{app}) for negatively charged POPC/POPG (75/25 mole/mole) monolayers is almost identical to that for electrically neutral POPC monolayers. For G_t the situation is similar; however, the binding constant for negatively charged monolayers is even slightly lower than that for electrically neutral monolayers. In the case of $G_{t\beta\gamma}$ the binding constant for negatively charged lipid monolayers is, in contrast, higher by a factor of ~30 than the binding constant for electrically neutral lipid monolayers. This suggests that the apparent binding constant results from a synergistic interaction (cf. ref *33*) between hydrophobic and electrostatic contributions

$$K_{app}(\text{POPC/POPG}) = K_h K_{el} \quad (7)$$

The electrostatic contribution (K_{el}) can be experimentally determined under the assumption that the hydrophobic contribution (K_h) corresponds to K_{app} (POPC)

$$K_{el} = K_{app}(\text{POPC/POPG})/K_{app}(\text{PC}) \cong \exp(-z_{eff}\Psi_0 F_0/RT) \quad (8)$$

where z_{eff} is the effective signed charge of the membrane contact region of the protein, Ψ_0 is the membrane surface potential, F_0 is the Faraday constant, and RT is the thermal energy. The effective charge of the protein in contact with the membrane was estimated as $z_{eff} = +2.7$ for $G_{t\beta\gamma}$, $z_{eff} \sim 0$ for $G_{t\alpha}$, and $z_{eff} = -0.5$ for G_t using a surface potential, $\Psi_0 = -30$ mV for POPC/POPG (75/25 mole/mole) monolayers, and taking into account the intrinsic lipid-binding constants of Na^+ ($K_0 = 0.6$ M^{-1}) and of Ca^{2+} ($K_0 = 18$ M^{-1}) (*43*) the latter being similar to that of Mg^{2+} (*44*). Inspection of the molecular model (Figure 6) allows a tentative correlation between the charge, z_{eff}, and the amino acid residues in contact with the membrane as summarized in Table 1 (cf. also Figure 6).

At pH 5.5 binding constants of $G_{t\alpha}$ and G_t (but not of $G_{t\beta\gamma}$) are larger than at pH 7.5. The increase in binding constants is partially due to an increase in surface activity of the two proteins with decreasing pH and, in addition, most probably to the protonation of His^{11} in the N-terminus of $G_{t\alpha}$. This points again to the importance of $G_{t\alpha}$ for membrane binding of G_t.

Divalent Cations Are Required for Hydrophobic Interactions of $G_{t\alpha}$ and G_t with Membranes. Despite the fact that $G_{t\alpha}$ and $G_{t\beta\gamma}$ are comparable in their number of charged residues (105 and 110) and their net charge (−10 and −12), the latter is surface-active in buffer solution at neutral pH (in the absence of salts), while the former is not. To transform $G_{t\alpha}$ into its surface-active form Mg^{2+} or Ca^{2+} ions are required. $G_{t\alpha}$ as well as G_t penetration into negatively charged and electrically neutral lipid monolayers depends on the presence of divalent cations in a concentration-dependent manner (0.1−1 mM). The fact that G_t only inserts into membranes if $G_{t\alpha}$ is activated by divalent cations further supports the important role of the α-subunit for binding of the heterotrimer. This finding is in agreement with the early observation (*15*) that G_t can be dissociated from the membrane in low ionic strength buffers.

The role of divalent cations is thus not only to modulate the electrostatic repulsion between $G_{t\alpha}$ and the negatively charged membrane surface, possibly by complex formation with the N-terminal sequence -Glu^8-Glu^9-Lys^{10} (cf. ref *45*), but also to induce the possibility for hydrophobic interactions of $G_{t\alpha}$ and G_t with the lipid membranes in general. In the case of recoverin (*46*) Ca^{2+} was shown to induce the protrusion of the myristoyl moiety hidden in a hydrophobic pocket of the protein in the absence of Ca^{2+}.

A myristoyl chain hidden in the absence of divalent cations could explain the high solubility of $G_{t\alpha}$, its lack of surface activity, and its inability to insert into lipid monolayers. It takes photoactivated rhodopsin in disk membranes and excess $G_{t\beta\gamma}$ (*47*) to transfer recombinant $G_{t\alpha}$ lacking the myristoyl to the membrane, suggesting that the main task of the myristoyl modification is membrane targeting.

The Secondary Structures of G_t in Solution and at the Membrane Surface Are Similar. The agreement between the CD spectra of $G_{t\alpha}$, $G_{t\beta\gamma}$, and G_t measured at pH 7.5 in the absence of salts and those simulated on the basis of the X-ray

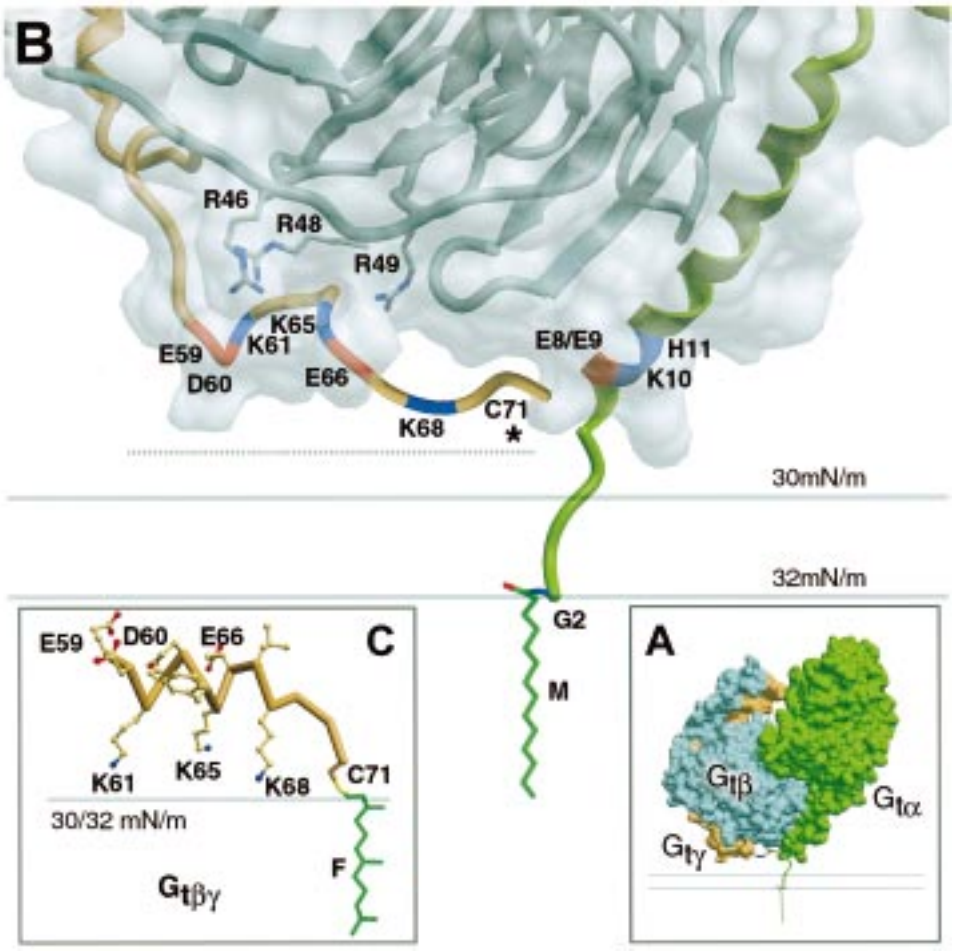

FIGURE 6: Molecular determinants responsible for membrane anchoring of G_t and its subunits as determined from binding experiments. (A) G_t in its crystal structure (*4*) at the membrane surface. (B) Membrane-binding region of G_t. The 4 N-terminal residues of $G_{t\alpha}$ and the 5 C-terminal residues of $G_{t\gamma}$, missing in the crystal structure, are added in an arbitrary (random) conformation, and a myristoyl chain (M) is attached at Gly^2 ($G_{t\alpha}$). The farnesyl chain attached at Cys^{71} ($G_{t\gamma}$) (*) is not shown, since its orientation in G_t cannot be determined, in contrast to its orientation in $G_{t\beta\gamma}$ (C). The two horizontal lines represent the position of the interface between the hydrocarbon and the headgroup region of a lipid membrane with a lateral packing density, $\pi = 30$ mN/m and $\pi = 32$ mN/m, respectively. $G_{t\alpha}$GDP provides the essential but not exclusive hydrophobic membrane anchor (cf. Discussion) consisting of the myristoyl chain, with (at 30 mN/m) and without (at 32 mN/m) approximately three N-terminal amino acid residues (or alternatively A3, A5, A7, not shown). The anionic residues E7, E8 (red) and residues K9 (cationic), H10 (cationic only at acidic pH) (blue) may constitute a Ca^{2+}-binding site in the presence of negatively charged lipid membranes. Residues K61, K65, and K68 of $G_{t\beta\gamma}$ do not contribute to the binding of G_t, possibly due to a larger distance to the membrane as compared to that in $G_{t\beta\gamma}$, indicated by stippled line (C). A slight tilt of G_t to the right-hand side could further increase this distance. (C) C-terminal sequence of $G_{t\beta\gamma}$ with a farnesyl chain (F) attached at C71. Sequence E59−K68 is modeled as an α-helix with residues K61, K65, and K68 oriented toward the negatively charged membrane surface and E59, D60, and E66 oriented toward the cationic residues, R46, R48, and R49, of $G_{t\beta}$. The figure was generated using DINO, a "Visualization System for Structural Data". A. Philippsen (1998) http: //www.bioz.unibas.ch/~xray/dino.

structure (*4*) provides evidence for a close similarity between the secondary structure in solution and that in the crystal as shown previously for another myristoylated, cytosolic protein (*33*). In contrast, a large difference between the two structures was observed for the transforming growth factor-β3 (*48*).

The influence of salts (100 mM NaCl (or NaF) and 1 mM $MgCl_2$), which have been shown to transform the highly water soluble $G_{t\alpha}$ into a surface-active compound and to increase the surface activity of G_t, is observed in CD spectra in terms of optical flattening (*38*) and light-scattering effects. They indicate protein association or micelle formation which has been observed previously for acetylated model proteins by means of light-scattering measurements (*40*).

The lack of spectral changes upon binding of G_t to POPC/POPG (75/25 mole/mole) vesicles (in the presence and absence of salts) at pH 7.5 shows that no large or overall change of secondary structure occurs upon membrane binding. Our monolayer insertion measurements show in addition that at most about 5% of the total amino acid residues located in the N-terminus of $G_{t\alpha}$ and the C-terminus of $G_{t\gamma}$ are involved in membrane binding (cf. Figure 6).

The difference between a local and an overall effect in G_t is best illustrated by a comparison of the process of membrane binding with that of glutamic acid (6% of the total amino acid residues) protonation. The latter process leads to an ellipticity increase of 12% at 217 nm which is due to the fact that the glutamic acid residues are distributed all over the protein.

The lack of an overall conformational change upon membrane binding allows one to use the crystal structure of the modified G_t (*4*) as a model for the membrane-bound native G_t (Figure 6A). The amino acid residues in the membrane-binding region that are missing in the crystal structure were added to the model, and the molecular

determinants of G_t and its subunits experimentally shown to be responsible for membrane recognition and anchoring are indicated in Figure 6B,C.

CONCLUSION

Divalent cations (~1 mM) are required to transform $G_{t\alpha}$-GDP into its surface-active, membrane-binding form. At 30 mN/m, $G_{t\alpha}$GDP is anchored by the myristoyl extension, most probably with a contribution of about three hydrophobic amino acid residues. At 32 mN/m $G_{t\alpha}$GDP seems to be anchored by the myristoyl extension only. Anchoring of $G_{t\alpha}$-GDP at negatively charged lipid monolayers shows an unusual sigmoidal surface pressure dependence in the narrow, physiologically relevant lateral packing density range of 29−31 mN/m. A similar behavior is observed for $G_{t\alpha}$GTPγS; however, the sigmoidal decrease occurs already between 26 and 27 mN/m. $G_{t\alpha}$GTP binding at bilayer packing densities is thus unmeasurably low, which is indeed known for disk membranes (*15*).

$G_{t\beta\gamma}$ is surface-active even in the absence of salts, suggesting a permanent exposure of the farnesyl extension to water. Anchoring at monolayers mimicking the negative surface density of disk membranes is due to the penetration of the farnesyl modification and is reinforced by 2−3 cationic charges which most likely correspond to the C-terminal lysine residues. Farnesyl anchoring shows little surface pressure dependence in the physiologically relevant range of membrane packing densities.

G_t anchoring at monolayers mimicking the negative surface charge density of disk membranes is primarily due to the hydrophobic anchor of $G_{t\alpha}$ with only a small hydrophobic contribution from $G_{t\beta\gamma}$. Whether the hydrophobic contribution of $G_{t\beta\gamma}$ arises from a partial insertion of the farnesyl modification or from the insertion of the carboxymethyl group of Cys^{71} cannot be decided on the basis of the present experiments. The latter mechanism would free the farnesyl chain for possible protein interactions. For example, it was recently shown that the farnesylated C-terminal peptide of Gγ interacts with the active receptor, rhodopsin (*49*).

The charged residues of $G_{t\beta\gamma}$ do not contribute to binding of G_t. Shielding of the charged residues could be simply due to a larger distance between the lysine residues in the heterotrimer and the membrane surface (Figure 6B). G_t exhibits a small electrostatic repulsive interaction, most probably arising from the N-terminal $Glu^{8,9}$ residues of $G_{t\alpha}$. In the absence of salts G_t repulsion from the membrane surface can thus be expected, which is in agreement with the early observation of ref *15*.

In summary, we have shown that the membrane recognition region of G_t contains the characteristic elements, required for reversible membrane binding by means of a myristoyl-electrostatic switch (cf. ref *50*). A simple version of a myristoyl-electrostatic switch triggered by minute pH changes around pH 7.0 was found previously for myristoylated hisactophilin (*33*). For G_t the situation is much more complex. The hydrophobic anchor basically consisting of a fatty acyl modification seems to be reinforced by hydrophobic amino acid residues of $G_{t\alpha}$ and a hydrophobic component of $G_{t\beta\gamma}$. The electrostatic element most probably consists of ($Glu^{8,9}$) and is triggered by divalent cations. The lack of surface activity of $G_{t\alpha}$ in the absence of divalent cations suggests the possibility of an occlusion of the myristoyl chain in a hydrophobic groove of the protein in the absence of salts and might enhance this effect.

The different dependencies on monovalent and divalent ions, on pH, and on the lateral packing density of the membrane observed for the heterotrimer and its subunits, $G_{t\alpha}$GDP, $G_{t\alpha}$GTP, and $G_{t\beta\gamma}$, provide the basis for highly sensitive and specific modulation mechanisms in the course of signal transduction.

ACKNOWLEDGMENT

We are very grateful to Ansgar Philippsen for generating the molecular models in Figure 6.

REFERENCES

1. Stankowski, S. (1984) *Biochim. Biophys. Acta 777*, 167−182.
2. Lambright, D. G., Noel, J. P., Hamm, H. E., and Sigler, P. B. (1994) *Nature 369*, 621−628.
3. Helmreich, E. J., and Hofmann, K. P. (1996) *Biochim. Biophys. Acta 1286*, 285−322.
4. Lambright, D. G., Sondek, J., Bohm, A., Skiba, N. P., Hamm, H. E., and Sigler, P. B. (1996) *Nature 379*, 311−319.
5. Kokame, K., Fukada, Y., Yoshizawa, T., Takao, T., and Shimonishi, Y. (1992) *Nature 359*, 749−752.
6. Neubert, T. A., Johnson, R. S., Hurley, J. B., and Walsh, K. A. (1992) *J. Biol. Chem. 267*, 18274−18277.
7. Fukada, Y., Takao, T., Ohguro, H., Yoshizawa, T., Akino, T., and Shimonishi, Y. (1990) *Nature 346*, 658−660.
8. Wedegaertner, P. B., Wilson, P. T., and Bourne, H. R. (1995) *J. Biol. Chem. 270*, 503−506.
9. Bigay, J., Faurobert, E., Franco, M., and Chabre, M. (1994) *Biochemistry 33*, 14081−14090.
10. Sternweis, P. C. (1986) *J. Biol. Chem. 261*, 631−637.
11. Audigier, Y., Journot, L., Pantaloni, C., and Bockaert, J. (1990) *J. Cell Biol. 111*, 1427−1435.
12. Mumby, S. M., Heukeroth, R. O., Gordon, J. I., and Gilman, A. G. (1990) *Proc. Natl. Acad. Sci. U.S.A. 87*, 728−732.
13. Linder, M. E., Pang, I. H., Duronio, R. J., Gordon, J. I., Sternweis, P. C., and Gilman, A. G. (1991) *J. Biol. Chem. 266*, 4654−4659.
14. Matsuda, T., Takao, T., Shimonishi, Y., Murata, M., Asano, T., Yoshizawa, T., and Fukada, Y. (1994) *J. Biol. Chem. 269*, 30358−30363.
15. Kühn, H. (1980) *Nature 283*, 587−589.
16. Seelig, A. (1987) *Biochim. Biophys. Acta 899*, 196−204.
17. Taschner, N. (1992) Diploma Thesis, Biocenter of the University of Basel, Basel, Switzerland.
18. Seelig, J., and Seelig, A. (1980) *Q. Rev. Biophys. 13*, 19−61.
19. Seelig, J., Seelig, A., and Tamm, L. (1982) in *Lipid−Protein Interactions* (Jost, P., and Griffith, O. H., Eds.) pp 127−148, John Wiley & Sons, Inc., New York.
20. Koenig, B. W., Strey, H. H., and Gawrisch, K. (1997) *Biophys. J. 73*, 1954−1966.
21. Litman, B. J., and Mitchell, D. C. (1996) *Lipids 31* (Suppl), S193−S197.
22. Demel, R. A., Geurts van Kessel, W. S., Zwaal, R. F., Roelofsen, B., and van Deenen, L. L. (1975) *Biochim. Biophys. Acta 406*, 97−107.
23. Kahlert, M., and Hofmann, K. P. (1991) *Biophys. J. 59*, 375−386.
24. Lamb, T. D., and Pugh, E. N., Jr. (1992) *Trends Neurosci. 15*, 291−298.
25. Iiri, T., Farfel, Z., and Bourne, H. R. (1998) *Nature 394*, 35−38.
26. Hubbell, W. L. (1990) *Biophys. J. 57*, 99−108.
27. Heck, M., and Hofmann, K. P. (1993) *Biochemistry 32*, 8220−8227.
28. Yamazaki, A., Tatsumi, M., Torney, D. C., and Bitensky, M. W. (1987) *J. Biol. Chem. 262*, 9316−9323.

29. Bradford, M. M. (1976) *Anal. Biochem. 72*, 248−254.
30. Fahmy, K., and Sakmar, T. P. (1993) *Biochemistry 32*, 7229−7236.
31. Antonny, B., Bigay, J., and Chabre, M. (1990) *FEBS. Lett. 268*, 277−280.
32. Seelig, A. (1992) *Biochemistry 31*, 2897−2904.
33. Hanakam, F., Gerisch, G., Lotz, S., Alt, T., and Seelig, A. (1996) *Biochemistry 35*, 11036−11044.
34. Yang, J. T., Wu, C. S., and Martinez, H. M. (1986) *Methods Enzymol. 130*, 208−269.
35. Fromherz, P. (1975) *Rev. Sci. Instrum. 46*, 1380.
36. Boguslavsky, V., Rebecchi, M., Morris, A. J., Jhon, D. Y., Rhee, S. G., and McLaughlin, S. (1994) *Biochemistry 33*, 3032−3037.
37. Evans, R. W., Williams, M. A., and Tinoco, J. (1987) *Biochem. J. 245*, 455−462.
38. Duysens, L. N. M. (1956) *Biochim. Biophys. Acta 19*, 1−12.
39. Peitzsch, R. M., and McLaughlin, S. (1993) *Biochemistry 32*, 10436−10443.
40. Pool, C. T., and Thompson, T. E. (1998) *Biochemistry 37*, 10246−10255.
41. Silvius, J. R., and l'Heureux, F. (1994) *Biochemistry 33*, 3014−3022.
42. Ptitsyn, O. B., and Finkelstein, A. V. (1983) *Biopolymers 22*, 15−25.
43. Macdonald, P. M., and Seelig, J. (1987) *Biochemistry 26*, 1231−1240.
44. Lau, A., McLaughlin, A., and McLaughlin, S. (1981) *Biochim. Biophys. Acta 645*, 279−292.
45. Hollosi, M., Urge, L., Perczel, A., Kajtar, J., Teplan, I., Otvos, L., Jr., and Fasman, G. D. (1992) *J. Mol. Biol. 223*, 673−682.
46. Ames, J. B., Porumb, T., Tanaka, T., Ikura, M., and Stryer, L. (1995) *J. Biol. Chem. 270*, 4526−4533.
47. Faurobert, E., Otto-Bruc, A., Chardin, P., and Chabre, M. (1993) *EMBO J. 12*, 4191−4198.
48. Pellaud, J., Schote, U., Arvinte, T., and Seelig, J. (1999) *J. Biol. Chem.* (in press).
49. Kisselev, O. G., Meyer, C. K., Heck, M., Ernst, O. P., and Hofmann, K. P. *Proc. Natl. Acad. Sci. U.S.A.* (in press).
50. McLaughlin, S., and Aderem, A. (1995) *Trends Biochem. Sci. 20*, 272−276.
51. Fischer, H., Gottschlich, R., and Seelig, A. (1998) *J. Membr. Biol. 165*, 201−211.

BI990298+